Sensing fiber selection for point displacement measuring with distributed optic fiber sensor

Zhang, Xuehui; Broere, Wout

DOI
10.1016/j.measurement.2022.111275

Publication date
2022

Document Version
Final published version

Published in
Measurement: Journal of the International Measurement Confederation

Measurement 197 (2022) 111275

Contents lists available at ScienceDirect

Measurement

journal homepage: www.elsevier.com/locate/measurement

Sensing fiber selection for point displacement measuring with distributed optic fiber sensor

Xuehui Zhang, Wout Broere *

Geo-Engineering Section, Department of Geoscience and Engineering, Delft University of Technology, Delft, The Netherlands

ARTICLE INFO

Keywords:
Distributed optical fiber sensor (DOFS)
Point displacement
Metrics of sensing fiber
Fiber selection
Parameter calibration
Relaxation

ABSTRACT

Distributed optical fiber sensors (DOFS) allow for distributed strain sensing and can be installed to function as extensometers for measuring point-displacements. This paper discusses the metrics of optimal sensing fiber selection for point-displacement measuring. Key metrics include the physical structure, mechanical parameters and light transmission coefficients. Calibration tests for verification of the optical fiber properties are designed and results of four fiber types are presented. Finally, creep and relaxation behavior of optical fibers is discussed based on manual tension test results, and a quantification model is proposed to assess the induced measurement error for sensing fiber. The maximum (absolute) measurement error for two common fiber types used in point displacement measurements is determined to be below 8%, and the study shows that pretensioning of the fiber helps to reduce such measurement errors.

1. Introduction

Sensors play a vital role in structural health monitoring, as they can provide the necessary information to make a detailed structural state analysis. Various types of sensors, including electrical strain gauges and Fiber Bragg Gratings (FBG), have been utilized by researchers and engineers to measure the structural response statically or dynamically. With continuous innovations more and more types of sensors are developed and applied in structure monitoring, and among them distributed optical fiber sensors (DOFS) are a class that offers the unique advantage of distributed sensing.

The working principles of DOFS are generally based on the optical phenomena of light scattering, optical loss, and polarization [1,2]. Among them DOFS based on Brillouin scattering is the most widely used commercial technique for strain and temperature sensing in structural health monitoring. When light propagates along the optical fiber, Brillouin scattering occurs where a part of the propagating light will be backscattered, and the photonic properties (wavelength, frequency, et al.) of the backscattered light are influenced by the fiber strain and temperature [1,3,4]. Technically, by analyzing the photonic property change (Brillouin frequency shift) of the light in the fiber, the distributed strain or temperature along the fiber axis can be measured. And if the optical fiber is attached to the target structure or material properly, a spatial-resolved strain or temperature measurement can be obtained.

Generally, a complete DOFS system consists of a sensing optical fiber plus a signal interrogator. The optical fiber is extended and attached to the monitored host structure (or material), and works both as a sensing part and signal transmission channel, while the fiber end (one end or both ends) is plugged into the interrogator for signal stimulation and processing. DOFS has many advantages over conventional electronic sensors, such as: (1) distributed sensing; (2) immunity to electromagnetic interferences; (3) the potential of long sensing distances of above a hundred kilometers [1,3]. Therefore, DOFS is more frequently used in civil engineering, including in monitoring buildings and bridge structures [5,6], pile foundations [7], tunnels and landslides [8,9,10], among others [11].

In civil engineering monitoring applications, DOFS is mostly used for distributed strain sensing and point displacement measuring. In distributed strain sensing, the optical fiber is bonded continuously on the structure's surface, or embedded into the structure (with a continuous bonding at the fiber-structure interface) to measure the distributed strain along the whole bonding length. Studies on distributed strain sensing can be found in Ohno et al. [5], Soga [9], Schwamb et al. [7], Pei et al. [11] and Pelecanos et al. [12]. In point displacement measuring, a short length optical fiber is fixed at two points, the interval fiber section between (referred as the gauge length, without bonding to structure) works as an extensometer and relative displacement (of the two fixture points) can therefore be measured. Since multiple gauge lengths can be

* Corresponding author at: Geo-Engineering Section, Delft University of Technology, CITG Building, Stevinweg 1, 2600 GA Delft, The Netherlands.
E-mail addresses: X.Zhang-10@tudelft.nl (X. Zhang), W.Broere@tudelft.nl (W. Broere).

https://doi.org/10.1016/j.measurement.2022.111275
Received 11 September 2021; Received in revised form 11 March 2022; Accepted 26 April 2022
Available online 30 April 2022

set up on a single long optical fiber cable, tens or even hundreds of extensometers are easily combined into a sensor-chain, and this can greatly reduce the complexity of a sensor network compared to conventional electrical extensometers. Therefore, DOFS is increasingly installed as extensometer to measure relative point displacements, like structural joint deformations [9,13,10] or crack widths [14]. For example, [13] used optical fiber sensors to detect joint openings, where the fiber gauge length is point-fixed to cross the tunnel circumferential joint. In another study [10], the optical fiber is used to instrument the segment circumferential joint of a shield tunnel.

However, previous studies mainly focus on field applications of DOFS on a project level, while limited attention is paid to the properties of the optical fiber itself. As an essential part of the setup, the optical fiber properties strongly affect the accuracy of the DOFS system. There are many optical fiber products available designed primarily for use in the telecommunication industry, but not all of them are directly suitable for deformation measuring. The quality standards or metrics for telecommunication optical fiber products, such as the fracture stress, or the durability in corrosion [15,16], are mostly focused on verifying the quality of bare optical fibers and do not fully cover the properties that are important for sensing purposes, as listed in 2.2 below. For point-displacement measuring, an improper fiber selection may result in measurement errors or even failure of the DOFS system. But the key questions are: (1) what metrics (of optical fiber) can be used to define a qualified sensing fiber and (2) how to calibrate the key metrics (or parameters) of potential sensing fibers. Despite the high potential of DOFS, there is no reference technical standard available for fiber quality verification and calibration for strain monitoring applications.

Besides, in point-displacement measurements, the optical fiber sensor tends to work on a much higher strain level (even above 1.0%) than in distributed strain sensing (mostly well below 0.5%) according to most published studies, such as maximum strain levels around 0.20% in Ohno et al. [5], 0.25% in Schwamb et al. [7] and 0.20% in Pelecanos et al. [12]. Under high working strain levels, many optical fibers have a tendency to creep or relax, which may cause significant measurement errors. The existence of creep at low-strain levels has been verified in several experimental studies [17,18,19], but creep or relaxation under high strains (around 1%, or even higher) and its effects on the DOFS system are not studied quantitatively, and there is no proposed model or methodology, theoretically or empirically, for evaluation of the measurement error induced by optical fiber creep.

In material science, creep generally refers to a slow continuous deformation of a material under constant stress (or loading) [20]. A common creep test for optical fibers is to fix the fiber at one end, while the other end is stretched by a constant load, and the tensioned fiber length (gauge length) can displace freely. Such standard creep experiments have been performed by Ding et al. [17] and Song et al. [19]. However, in point displacement monitoring, the optical fiber sensor is normally fixed at both points (with no free end) and deforms along with the host structure. In those conditions, stress relaxation when the optical fiber is continuously stretched (at a given strain level) is a more important issue to consider, as this may lead to a shift from elastic (recoverable) to plastic (non-recoverable) strain, which is of course a different phenomenon than an ongoing strain increase under a constant load (creep). Although relaxation behavior of the optical fiber (at tension) is closely related to the creep behavior, the general creep test in previous studies is unable to capture the actual behavior of optical fiber sensors in deformation measuring.

As DOFS applications for point-displacements are expected to boost significantly, it is highly necessary to reflect on the potential metrics for sensing fiber selection, to study the strain behavior of optical fiber in a practical monitoring context, and to build a quantitative model to describe the creep and relaxation properties, to assess the induced measurement error and to provide mitigation measures to reduce its effect on the DOFS system.

This study focuses on the technical metrics and selection of sensing fibers for point displacement measuring. The metrics of optimal sensing fiber are discussed and summarized first, and standard calibration methods for verifying important fiber parameters are proposed. To illustrate the fiber calibration procedures, test results of four types of optical fiber are presented in detail. Finally, a quantitative model is put forward to describe the creep or relaxation properties of optical fiber (at given strain level) based on the calibration test results, and the maximum relative error (caused by fiber relaxation) of DOFS in measurement is assessed by the proposed model.

2. Metrics of sensing fiber

2.1. General structure of optical fibers

In a DOFS system, the optical fiber is attached to the monitored structure, working as both sensor and signal transmission channel. Property verification and calibration are necessary before deciding on a suitable sensing fiber type. A good understanding of fiber properties is the prerequisite for proper sensing fiber selection. The number of available fiber types made specifically for strain sensing is limited, and although the fiber cable types applied in the telecommunication industry are quite extensive, none of them are ideal for sensing purposes. Until now there is no reference technical standard published for quality verification of potential sensing fibers, which is a disappointment for DOFS users. Therefore, to study the key metrics of optimal sensing fibers, is important for reliable DOFS application.

Single-mode fiber is preferred over multi-mode fibers in distributed sensing, as the latter has a higher signal attenuation and a lower sensing distance. In the optical fiber manufacturing industry, a general basic product is the 0.25 mm-in-diameter bare fiber (D-0.25 mm), e.g. by Corning [24]. This bare fiber has an internal silica core with an outer diameter of 8–9 μm, a cladding with an outer diameter of 125 μm and external coating with an outer diameter of 250 μm. Generally, the core plus cladding forms the route for light transmission and hence they are the actual “sensing part” of the fiber. The basic D-0.25 mm bare fiber product from primary-level optical fiber manufacturers (like Corning, OCC, and others) are further processed (adding reinforcement parts and strong external protection jackets) by secondary-level manufacturers to make robust fiber cables for industry use. Another basic fiber product is the 0.9 mm-in-diameter fiber (D-0.9 mm) made from the D-0.25 mm by adding an external polymer jacket, as shown by Ding et al. [17]. The D-0.9 mm fiber can be processed to make tight-buffer or loose-buffer strong fiber cables for indoor and outdoor use, see Fig. 1.

It should be mentioned that the physical structure of the fiber generally decides the strain transfer between the internal fiber core and external jacket layer. The majority of single-mode optical fiber cables, both in telecommunication or sensing, are made from the D-0.25 mm bare fiber or the D-0.9 mm fiber by adding an additional external jacket, sheath, or reinforcement parts (wire/strand/metal mesh) as protection, and therefore the optical fiber cross-section has a layered structure (in radial direction), as shown in Fig. 1. The inter-layer shear transfer determines whether the external strain can be transmitted into fiber core and hence be sensed.

Generally, tight-buffered fiber assures strong inter-layer bonding, and very limited slippage (between the internal fiber core and external jacket) occurs when strained (under normal working strain level). A type of tight-buffer optical fiber (with an outer diameter of 2 mm) is shown in Figs. 1(a) and 2. In contrast, loose-buffered optical fiber allows relative inter-layer slippage and hence very weak strain transfer, see Figs. 1(b) and 2. Therefore, strain sensing fiber should be tight-buffered, while loose-buffered fiber is more used for temperature measurement.

2.2. Metrics for sensing fiber selection

The key metrics of potential sensing fibers are proposed and listed as below:

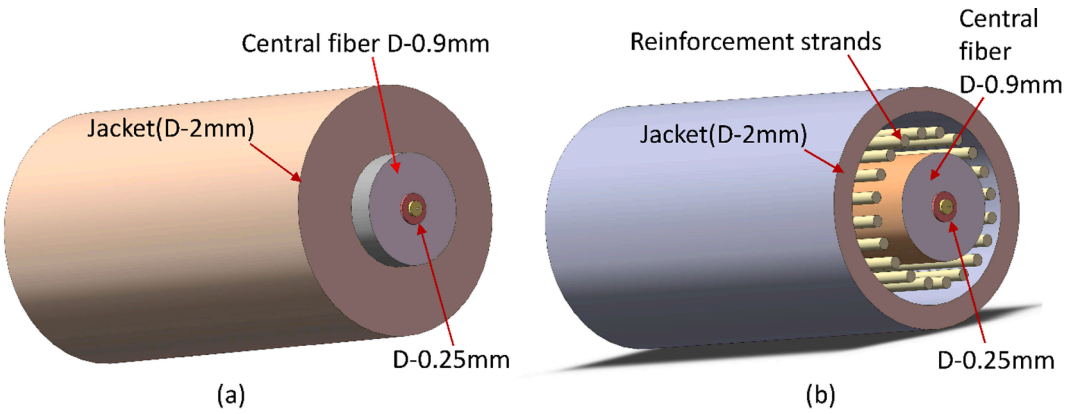

Fig. 1. Physical structure of fiber: (a) tight-buffered and (b) loose-buffered.

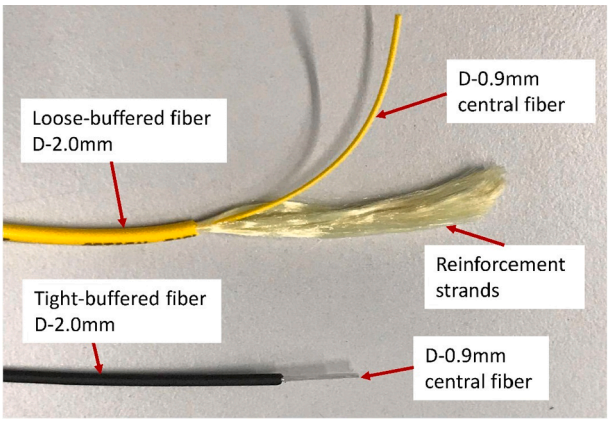

Fig. 2. Tight-buffered and loose-buffered optical fiber.

(1) The maximum working strain (MWS)

The maximum working strain (MWS) refers to the maximum strain sustained by an optical fiber where no (significant) relaxation occurs. For tight-buffered sensing fibers, MWS is strongly related to the material properties of the glass core, coating and jacket, and the interface bonding strength. Some researchers proposed to use the elastic limit strain from the fiber stress–strain curve as a metric [21], but the precise fiber stress is not straightforward to determine as the shrinkage of the optical fiber cross-section is usually quite significant when the fibers are tensioned.

A preferred method to define the MWS of optical fibers in deformation monitoring is to directly measure the Brillouin frequency shift (BFS) and the imposed strain (hereafter referred as strain unless otherwise specified). Within the MWS range, the Brillouin frequency shift (BFS) vs strain ($f-\varepsilon$) curve of the fiber maintains a high degree of linearity under loading–unloading (or tension/de-tension) cycles. When the optical fiber is tensioned beyond the MWS, the fiber usually creeps significantly, and serious inter-layer slippage may occur if the tension is sustained, which causes unacceptable errors for strain sensing applications. It should be noted that in some fiber types, creep may occur even under very low strain levels, and the MWS can be defined as the sensing range within which the measurement error (by creep or relaxation) remains limited (for example, below 10%). The MWS can for instance be measured by a cyclic tension test, as discussed below.

(2) The limit strain

The strength of the optical fiber is an important parameter for general fiber products. The limit strength (described either as a maximum fiber stress or strain) of optical fibers has been extensively studied by researchers [15,16,21]. When used for sensing purposes, it is more practical to express this as the limit strain, which is the maximum strain an optical fiber can reach before breaking, leading to either partial (usually the jacket) or full rupture of the fiber cross-section.

Note that rupture of the jacket will expose the very fragile central fiber, which makes the sensing fiber quite vulnerable. A full cross-section breakage, even at a single point along the fiber, usually results in a full failure of the whole distributed sensing network (although single-end measuring may be still possible, but at significantly reduced accuracy). Therefore, it is important for DOFS users to make sure the limit strain should not be reached under normal working conditions, so as to maintain a continuous robust signal transmission.

(3) Relaxation potential

Relaxation is the phenomenon that the stress level in an optical fiber, when subjected to a constant strain, tends to (partially) decrease over time. This can be described by a shift of elastic (recoverable) to plastic (non-recoverable) strain and as such relaxation is closely related to the creep that the optical fiber would undergo when subjected a continuous (even if not constant) tensile force. Therefore, a (standard) creep test can help to indicate the relaxation potential of the sensing fiber, but a calibrated tension test (imposing a given strain) is preferred when analyzing the potential measurement errors in deformation measuring.

A good sensing fiber shall not show significant relaxation behavior when tensioned below the maximum working strain (MWS). It must be mentioned that almost all tight-buffered optical fibers with polymer jackets show signs of creep and relaxation, but what matters is to what extend this affects the measuring accuracy. Note that the Brillouin frequency shift (BFS) is linear to the actual optical fiber strain. If the BFS and the corresponding imposed strain of the optical fiber are measured simultaneously, relaxation will result in a hysteresis loop in the BFS-strain ($f-\varepsilon$) curve in a loading–unloading process, which may cause unacceptable errors when translating measured BFS to actual strain. Relaxation behavior of sensing fibers and their effects on DOFS measurement will be discussed in more detail in Section 4.

(4) The strain sensitivity coefficient

The strain sensitivity coefficient (at a given light wavelength) relates the measured BFS to imposed strain [4,3] and is an important parameter which needs to be well calibrated. In a tension test, the BFS-strain curve can be obtained, and generally the gradient of a linear fit line is determined as the strain sensitivity coefficient. In previous studies, the strain coefficient generally lies between 40 and 50 MHz/0.1% [5,21,10].

(5) The temperature sensitivity coefficient

The temperature sensitivity coefficient (at a given light wavelength) relates the BFS to temperature change [4,3] and is measured usually by a warm-bath experiment, where a loose fiber is immersed into warm water or liquid. Based on the fitted temperature-BFS curve the temperature sensitivity coefficient is obtained. However, according to some previous studies, determining the temperature sensitivity coefficient accurately may not be strictly necessary if the temperature effects can be appropriately compensated for, for example by setting up an additional loose fiber section (a zero-strain section) very close to the sensing fiber section (the strained section), and the measured BFS change of the zero-strain section will show the temperature influence which needs to be compensated for. Such methods can be seen in Gue et al. [13] and Lienhart et al. [22].

(6) Axial stiffness of sensing fiber

The axial stiffness of sensing fiber EA (where E denotes the elastic modulus of the fiber and A the cross-sectional area) is an important metric which could generally be used to estimate the fiber's robustness to external impacts [21]. A high axial stiffness usually also indicates the fiber can withstand large axial tension forces and does not break easily. The axial stiffness is mostly determined by the reinforcement parts (sheaths or reinforcement strands) of the fiber cross-section. For optical fibers used in harsh field environments (say embedded into concrete or ground), the central fiber may be wrapped with longitudinal reinforcement metal strings or wires, and hence a high axial stiffness can be achieved. The axial stiffness of some potential optical fibers for strain sensing applications are shown in Table1.

However, it should be mentioned that whereas a high axial stiffness can be beneficial to create a sturdy and protected fiber, it also makes the fiber tensioning and sensor installation quite difficult or even impossible, which is especially troublesome when manual pre-tensioning is needed during sensor installation. Therefore, selection of a DOFS fiber requires balancing between axial stiffness and ease of installation in different monitoring setups. The axial stiffness can be checked in a fiber tension test, such as in Iten et al. [21]. In general, keeping the ease of sensor installation in mind, it holds that:

(1) usually, bare fibers (D-0.25 mm) and D-0.9 mm tight-buffered fibers are very fragile (especially in bending) and are not highly recommended to be used directly in harsh environments unless reliable protection is provided.
(2) an axial stiffness of no more than 3 kN is preferred for manual pre-tensioning above 0.5% strain, for instance when the fiber is used as an extensometer in point displacement sensing.
(3) an axial stiffness of no more than 5 kN is preferred for manual pre-tensioning below 0.30%, for cases where the fiber is embedded into concrete walls or piles for distributed strain sensing.
(4) even higher stiffness (of above 5 kN) is acceptable when manual pre-tensioning is not needed during installation, for example when burying the fiber into the ground directly for landslide detection. However, measurement sensitivity should also be considered in these monitoring cases, as too stiff a fiber may debond easily from the surrounding soil. More information on fiber installation for such cases can be found in Iten et al [8].

Table1
Axial stiffness of some potential optical fiber.

Fiber type	Outer diameter	Axial stiffness
SMF bare fiber by Corning Co.	0.25 mm	About 1 kN
TPEE tight buffered fiber by Nanzee Sensing Co.	0.9 mm	About 1 kN
Polyurethane tight buffered fiber by Nanzee Sensing Co.	2 mm	About 3 kN
Polyamide & metal protected fiber From Iten et al. [21]	3.2 mm	About 60 kN

3. Calibration tests of sensing fiber

3.1. Combined tension test

A combined tension test is the easiest way to verify both the mechanical properties and strain sensitivity of a sensing fiber. A typical calibration test can be set up on a tension machine, where a short fiber length is fixed at two points and tensioned step by step. The fiber ends are connected to the interrogator and the Brillouin frequency shift (BFS) corresponding to each loading step can be obtained, see Fig. 3. From the imposed strain and tension force the BFS-strain ($f-\varepsilon$) curve and force-strain (F-ε) curve can be obtained, from which the strain sensitivity coefficient and axial stiffness can be derived by a linear fit, see Fig. 3.

When executing the combined tension test, small strain increments per loading step (for example 0.05%) should be imposed preferably, so as to detect the maximum working strain, and potentially the limit strain, as accurately as possible in a loading test cycle. Ideally, load-unload cycles are conducted at pre-determined strain levels, for example 0.25%, 0.5%, 0.75% and 1%, to verify the possible relaxation of the fiber as well, in addition to the normal test procedures for determining the mechanical properties and strain coefficient as described by Lienhart et al. [22]. The relaxation behavior will be further studied in Section 4. For a qualified sensing fiber, there should be limited relaxation (to be determined by the fiber property and monitoring requirements) before reaching a certain strain level, and this strain level can be established as the maximum working strain (MWS).

3.2. Manual tension test

For sensing fibers used in point displacement measuring applications, the axial stiffness is generally not too high and hence a manual tension test could also work. Calibration can be conducted with reduced difficulty on a simple tension platform, where a short fiber length is anchored at two ends using glue (or clamps), see Fig. 4. In the tension test, one anchorage is not permanently fixed and can be translated, while the other end is fixed on the sliding platform. Two dial-gauges are attached to measure the imposed displacement and avoid in-plane tilting of the movable anchorage. The fiber ends are then connected to the interrogator for BFS measurement. Using this type of set-up multiple sensing fibers can be tested simultaneously.

The fiber fixation at the anchorages must be checked to be strong enough to resist possible slippage, which point of attention equally holds for a combined tension test using the tension machine. Generally, the fiber can be fixed either by physical clamping or by gluing. At high strain levels (for example, above 0.8% strain), the fiber cross-section tends to shrink noticeably, which can possibly cause debonding at the fiber-glue interface, or lead to small slippage at the fiber-clamp interface. In the laboratory calibration test, fiber debonding or slippage can be checked visually. A reliable anchorage method shall not cause significant debonding or slippage at the anticipated working strain levels, and it is strongly suggested to fix the fiber in the tension test with the same method used afterwards in the field sensor installation.

3.3. Tension test results analysis of optical fiber

To illustrate the impact of different fiber types on the fiber parameters, the results of a laboratory manual tension test of several potential sensing fibers are presented here. In this test, five fiber lengths of four different types are fixed at a horizontal platform, see Fig. 5. Two dial-gauges are used to measure the displacement, and the imposed strain at each tension step is calculated. Each fiber length is set at 80 cm, and point fixed by epoxy glue at the anchorage plates (with a bonding length of 4 cm).

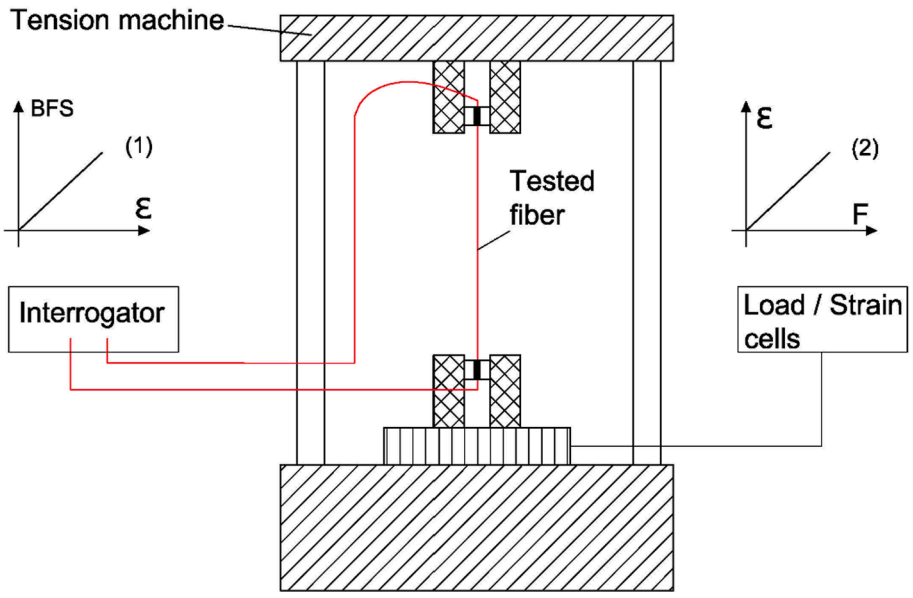

Fig. 3. Schematic of fiber calibration test on a tension machine.

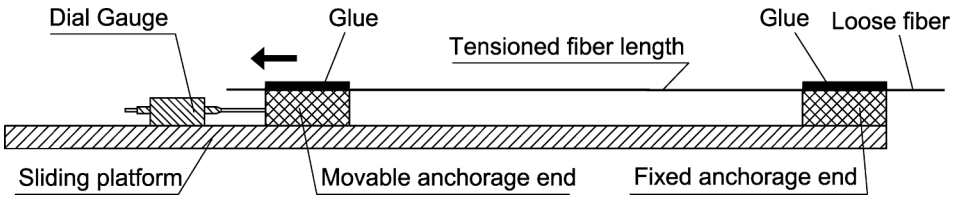

Fig. 4. Manual tension test platform.

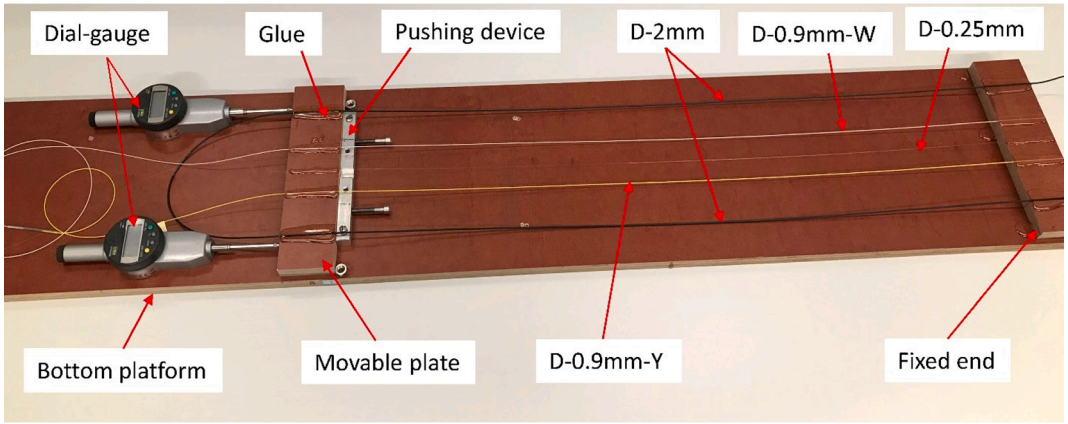

Fig. 5. Fiber calibration by manual tension test.

The tested sensing fiber types are:

(1) a polyurethane sheath tight-buffered fiber, typed NZS-DSS-C07 with a diameter of 2 mm (D-2 mm), manufactured by Nanzee Sensing Co. from Suzhou, China;
(2) a thermoplastic polyester elastomer (TPEE) sheath fiber typed NZS-DSS-C09 (2019-batch) with a diameter of 0.9 mm (white colored sheath, indicated as D-0.9 mm-W in Fig. 5), also manufactured by Nanzee Sensing Co.;
(3) a tight-buffered fiber with a diameter of 0.9 mm (yellow color, indicated as D-0.9 mm-Y in Fig. 5), which is obtained from the central fiber of a loose-buffered cable product typed AE001D-SLA9YR (see Fig. 2), manufactured by OCC, USA. From this fiber type with an outer diameter of 2 mm and a D-0.9 mm tight-buffer central fiber, the external loose jacket is peeled off and removed carefully and only the 0.9 mm central fiber is used for testing;
(4) a bare fiber with a diameter of 0.25 mm (D-0.25 mm), typed Corning SMF-28, manufactured by Corning Co., USA.

In the tension test, the four different fiber types are fusion-spliced (as they have the same fiber core dimension) to form a continuous fiber cable and both ends are connected into a Brillouin Optical Frequency Domain Analyzer (BOFDA) interrogator. This BOFDA, type fTB2505 and manufactured by fibrisTerre Systems GmbH, is used to measure the Brillouin frequency shift of the tensioned fibers at each loading step. It has a stated spatial resolution of 0.2 m (up to 1 km), a spatial accuracy of

0.05 m, and strain accuracy of 2με (0.0002%), according to fibrisTerre [23].

Another important aspect in the tension test is to determine the loading history. This experimental study targets to: (1) obtain the maximum working strain (the strain level below which no significant relaxation occurs); (2) analyze the strain behavior in a tensioned state (if significant relaxation is observed) and (3) detect possible residual strain when the optical fiber is fully de-tensioned. Previous studies have shown that the limit strain of a typical bare fiber (D-0.25 mm) is around 1.2% [21], and optical fiber generally exhibits only minimal creep behavior at strain levels below 0.20% [5,7], which indicates the behavior of optical fiber with strain between 0.25% and 1.2% is of most interest here. In the tension test, loading–unloading cycles are conducted at strain levels of 0.25%, 0.5%, 0.75%, 1% and 1.2%, see the loading cycles in Fig. 6. The five strain gradients are set in order to better verify the potential of relaxation and determine the MWS of each fiber type, with the impact of relaxation analyzed using the directly measured BFS. The temperature effects in the experiment period are compensated for by recording the BFS change of the loose section of each fiber type.

Fig. 7 shows the BFS-strain curve of the D-0.25 mm bare fiber under different loading cycles. From the results, it can be seen the bare fiber shows little relaxation (A BFS reduction of about 1 MHz) under a strain of 0.25%, but in the loading cycle of 0.50%, there is a permanent BFS reduction of about 4 MHz, which is induced by a very small permanent slippage (<0.01%). In the third loading cycle, the BFS-strain curve remains a highly linear with no sign of relaxation below 0.65% strain. However, coating breakage occurs at 0.7% strain and significant slippage was found between the coating and cladding layer, see Fig. 8(a). In the subsequent loading cycles (cycle-1.0% and 1.2%), the fiber core and cladding do not rupture (after a large unloading due to the slippage), and data-taking can be continued. Based on a linear fit of the BFS-strain curve (between 0% and 0.65%), the strain sensitivity of this D-0.25 mm bare fiber is about 47.40Mhz/0.1%. The relaxation potential of this fiber is very small and hence its effects can be neglected.

According to the test results, the maximum working strain of this D-0.25 mm bare fiber is about 0.65%, while the limit strain is about 0.7% at which strain coating breakage occurs (and although the signal transmission is continued, the exposed core and cladding are too fragile and can break quite easily). Note this bare fiber is very fragile and would rarely be used for field strain sensing applications, unless reliable protection is provided.

Fig. 9 shows the BFS-strain curve of the D-0.9 mm-Y fiber (yellow-jacket, as shown in Fig. 5) under cyclic loading. At each cycle, the load is imposed rapidly until it reaches the maximum strain (2 mins. per load step) and the fiber strain is sustained until the rate of BFS decrease (caused by relaxation) is below 0.4 MHz per hour. Then the fiber is unloaded to zero strain rapidly. Therefore, it is assumed the relaxation within a cycle occurs at the maximum load (the highest imposed strain). From Fig. 9 it can be seen the load-unload process results in a hysteresis loop in the BFS-strain curve, which indicates relaxation occurs when tensioned even at a low strain level of 0.25%. Unlike the D-0.25 mm fiber which exhibits a small amount of relaxation, this fiber shows quite significant relaxation behavior, which may affect the measurement results. The BFS reduction caused by relaxation are: (1) 6.4 MHz at 0.25% after 16 h; (2) 25.4 MHz at 0.50% after 66 h; (3) 48.8 MHz at 0.75% after 42 h; and (4) 47.1 MHz at 1.0% after 61 h.

Also, it can be observed in Fig. 9 that the loading and unloading curves for each cycle are highly parallel (with a very similar gradient), which indicates that every load cycle generates additional residual plastic strain in the fiber. The relaxation of this D-0.9 mm-Y fiber is mainly due to inter-layer slippage and creep of the jacket. In the subsequent load stages, the fiber jacket breaks at 1.1% strain and large inter-layer slippage occurs, which result in a sharp reduction of the measured BFS, see Figs. 8(b) and 9. The limit strain of this fiber is obtained as 1.1%, while at normal working strain level significant relaxation occurs. The measurement error caused by this relaxation will be discussed in the next Section.

The D-0.9 mm-W fiber (white-jacket, as shown in Fig. 5) shows similar relaxation behavior under tension as the D-0.9 mm-Y fiber does. Fig. 10 shows the BFS-strain curve of the D-0.9 mm-W fiber under cycle-0.75% and 1.0%, and as can be seen the BFS decrease is quite significant. The result of five load cycles is shown here and discussed in detail in Section 4. It can be seen that relaxation behavior of the D-0.9 mm-W fiber is actually different to that of the D-0.9 mm-Y fiber, as there exists a significant gap between the unloading curve of cycle-0.75% and the loading curve of cycle-1.0%. This gap indicates partial recovery of the residual strain after unloading.

To better illustrate the relaxation behavior, recoverable or elastic strain is defined here as that portion of the strain that is recovered or reversed over time after unloading (to zero strain), whereas the plastic strain, once it has occurred, will not be recovered. This is distinct from the instant portion of strain reversal that occurs directly after unloading, as the elastic strain reversal occurs over a similar time period as the initial strain.

That recoverable elastic strain occurs is also verified in Fig. 10, where a BFS increase is detected during the unloading process of cycle-1.0%. This increase of measured BFS is due to the elastic relief over a 98hrs period at a fixed strain of 0.35%. The dotted line indicates the

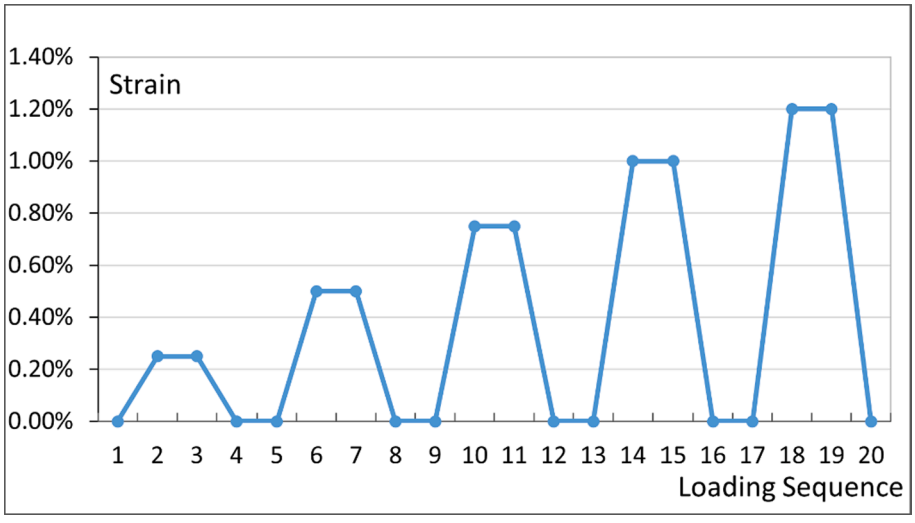

Fig. 6. Loading cycles for fiber calibration.

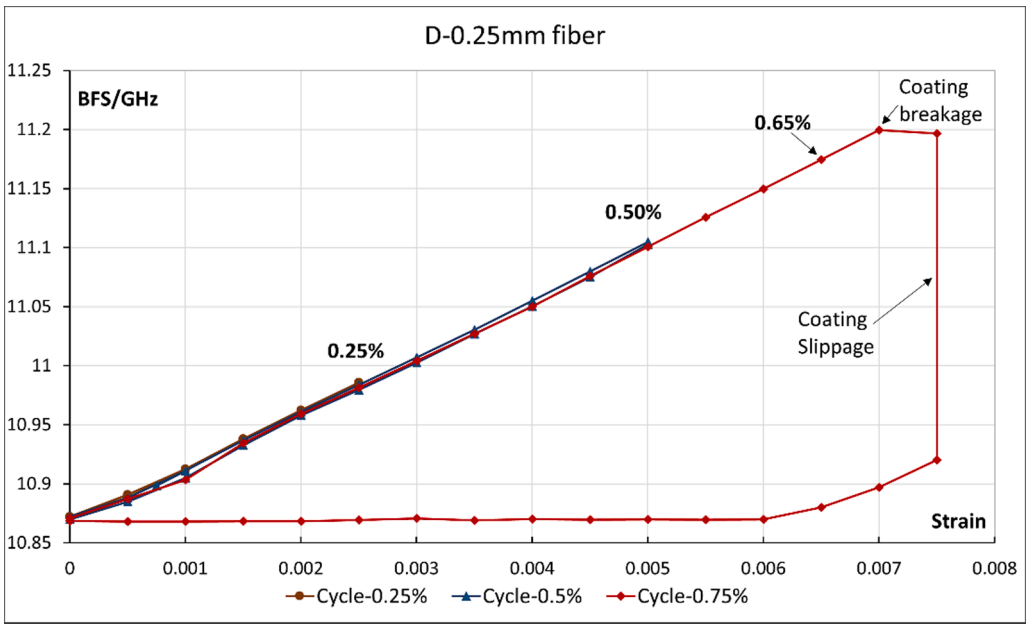

Fig. 7. Cyclic loading of D-0.25 mm bare fiber.

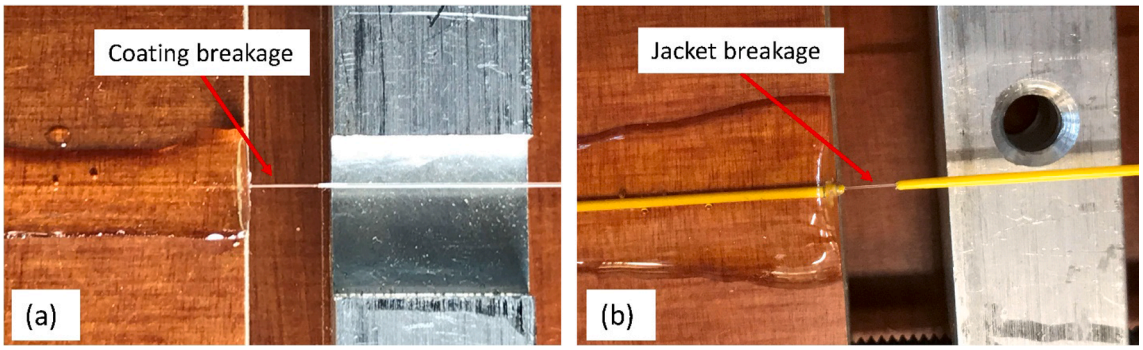

Fig. 8. Fiber breakage at limit strain:(a) D-0.25 mm bare fiber and (b) D-0.9 mm-Y fiber.

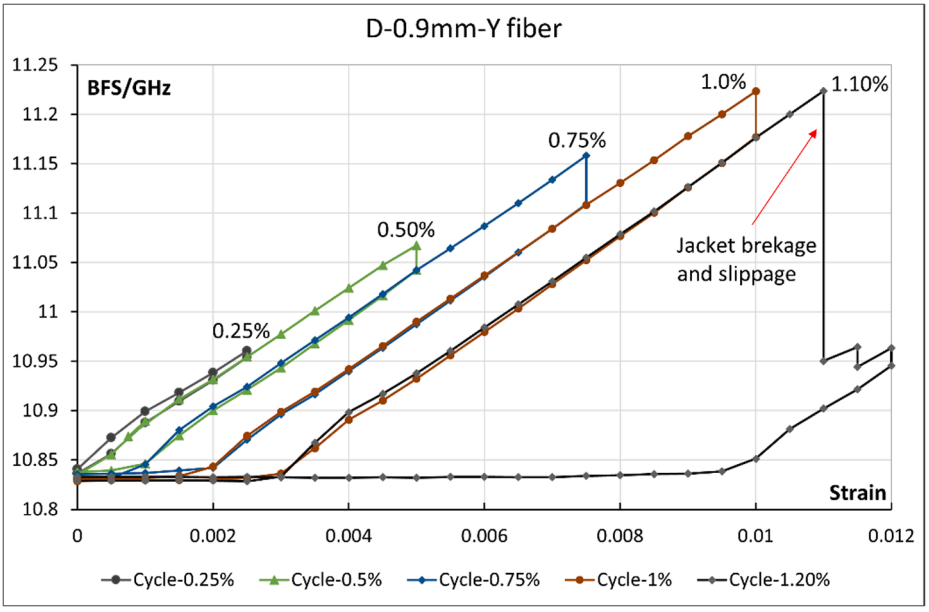

Fig. 9. Behavior of D-0.9 mm-Y fiber under cyclic loading.

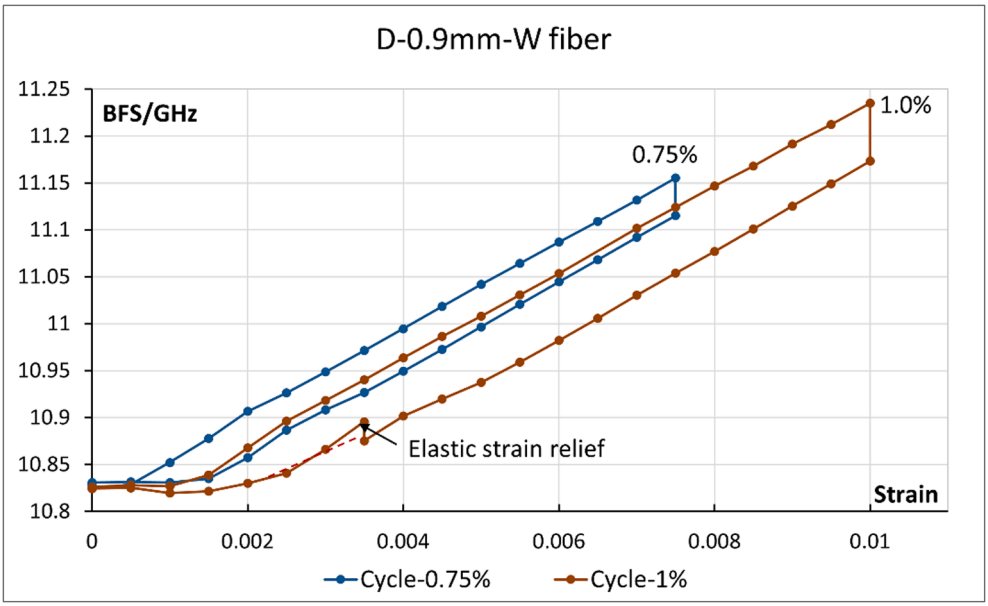

Fig. 10. Behavior of D-0.9 mm-W fiber (Cycle-0.75% and 1.0%).

most likely unloading curve under a fast unloading scenario (when no time lapse is set for elastic creep relief). The behavior of this fiber type is probably related to creep of the sheath material or inter-layer debonding. In the subsequent loading to 1.2%, sheath breakage was not found, and hence the limit strain is verified to be no smaller than 1.2%.

Fig. 11 shows the BFS-strain curves of the D-2 mm fiber under five successive load cycles. From the results, it can be seen the fiber keeps a highly linear response even under an imposed tension of 1.2% (the actual fiber strain is found to be about 1.25% due to a primary tension at baseline status), and shows very little creep behavior (a BFS reduction of less than 1 MHz is observed in each load cycle, except at cycle-0.5%, where a BFS increase of 3 MHz in 66 h at 0.50%, which is most probably due to a system error in signal interpretation). Based on a linear fit of the BFS-strain curve (between 0% and 1.2%), the strain sensitivity of this D-2 mm fiber is about 48.40 MHz/0.1%. The maximum working strain is verified to be above 1.20% and, among the four types of fiber tested in this test, this D-2 mm fiber is the most qualified type for strain sensing applications outside of lab conditions.

According to the calibration tension test, the D-2 mm fiber is the most suitable type for point displacement measuring, considering it has the lowest relaxation effects and the highest maximum working strain (MWS) among the four tested types of fiber. The D-0.25 mm bare fiber also has potential in measuring point displacement applications but at a reduced MWS of 0.65% (or even lower to obtain some safety margin) and under delicate protection. Both of the D-0.9 mm fiber types show significant relaxation that introduces measurement errors if they are used directly without any beforehand processing. These results show it is possible to select a potential sensing fiber which shows little relaxation or creep and calibrate the parameters using the proposed manual tension test. However, considering the possible sources resulting in relaxation, such as randomness in fiber manufacturing quality control or improper handling during the fiber transportation and field installation, even some specially made sensing fibers still show creep behavior, see [21]. Therefore, it is still reasonable and necessary to quantitatively analyze the relaxation behavior of optical fibers to be able to verify the validity of field measurements.

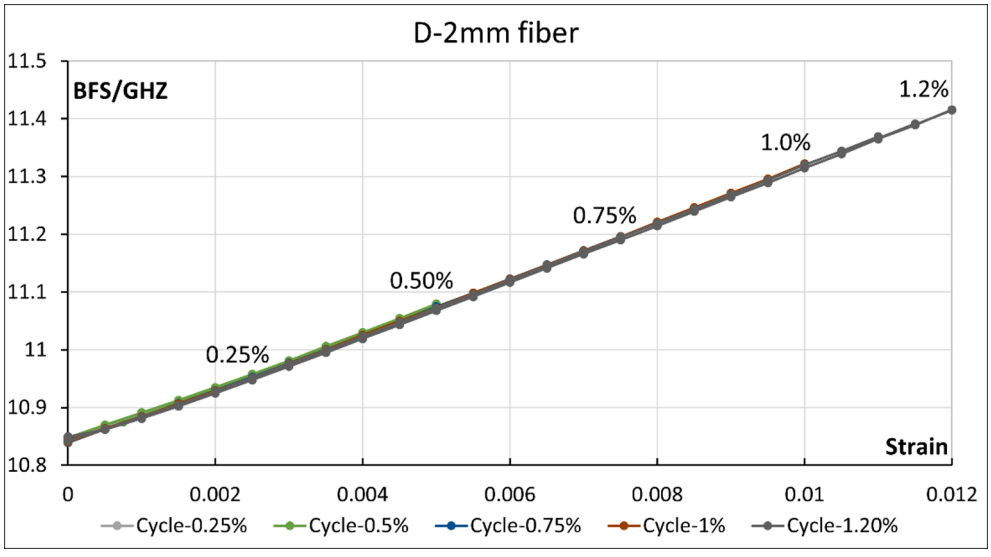

Fig. 11. Behavior of D-2 mm fiber under cyclic loading.

4. Relaxation analysis of sensing fiber

4.1. Introduction of fiber relaxation

According to the calibration tests shown in Figs. 9 and 10, tight-buffered optical fiber (cable) may show significant relaxation behavior in a tensioned state. When a fiber gauge length is pre-strained at installation, relaxation will result in a reduction of the measured BFS, and hence a smaller measured strain than the actual imposed strain (by the host structure). Therefore, relaxation affects the measurement accuracy of DOFS and should be studied carefully. Usually, the silica glass fiber core is less likely to significantly creep, but the outer protection jackets, especially when they are made of plastic or polymer material, have a higher tendency to creep under tension [17]. Also, inter-layer bonding may be not always assured due to difficulties in manufacturing process control, and this may result in relaxation of the tensioned fiber as well.

For a strained fiber length that is fixed well at both ends, the relaxation mainly comes from (1) the inter-layer slippage due to inadequate interface bonding and (2) creep of the external jacket material. Inter-layer bonding is the key for strain transfer and sensing, but when the bonding is not strong enough, inter-layer slippage may occur, which results in a permanent decrease of measured strain. Slippage may occur at the coating-cladding interface, or jacket-coating interface, see Fig. 1. For ordinary telecommunication fibers, the interface bonding may not be strong enough and slippage may occur even at very low strain levels, which is also shown by Ding et al., [17] and Song et al. [19]. Creep of the external jacket is highly related to the material properties. According to the tension test results in this study, the relaxation due to jacket creep consists of plastic and elastic components, where the plastic strain is unrecoverable whilst the elastic strain can recover over time after the strain is unloaded. Therefore, the total fiber strain decrease ε_t (by relaxation) can be expressed as Eq. (1):

$$\varepsilon_t = \varepsilon_s + \varepsilon_j = \varepsilon_p + \varepsilon_e \tag{1}$$

where ε_s is the strain by inter-layer slippage; ε_j is the strain by creep of the jacket material; ε_p is the total plastic strain, which consists of ε_s and the plastic component of ε_j; ε_e refers to the elastic component of ε_j.

For both ordinary telecommunication fibers and special-made sensing fibers, relaxation is always possible and should be well checked in the calibration test before using for monitoring tasks. Optical fibers which show relaxation may still have potential for strain sensing use, but the key issues are: (1) the amount of relaxation; (2) how to estimate the measurement error due to relaxation; and (3) what measures can be taken to reduce such measurement error? As mentioned in Section 3, fiber relaxation behavior can be verified by a cyclic tension test, since it will result in a hysteresis loop in the loading–unloading curve as shown in Fig. 10.

4.2. Description of relaxation properties based on tension test results

To illustrate the typical relaxation behavior of an optical fiber, the cyclic tension test results of the D-0.9mm-W fiber are firstly presented here in Fig. 12. In the tension test, five loading cycles are conducted, with the maximum strain imposed successively being 0.25%, 0.5%, 0.75%, 1.0% and 1.2%. The BFS-strain history curve shows that: (1) relaxation occurs, though not very significantly, during the first loading cycle to 0.25% strain; (2) significant relaxation occurs in the second loading cycle to 0.5% strain, and a highly identified hysteresis loop is present; (3) the total plastic strain due to relaxation accumulates and becomes larger in the subsequent load cycles with increased strain imposed (from 0.5% to 1.2%); (4) for a given loading cycle (for example the cycle-1%), the corresponding relaxation could be fully triggered (with a time delay) when the fiber is pre-tensioned (to 1%), and can be removed as a contributing factor in subsequent load cycles, which indicates that pre-tensioning of the fiber can potentially reduce the measurement errors introduced by relaxation.

What's more, it should be mentioned that the elastic strain component is recovered gradually during the unloading process, as can be seen in Figs. 10 and 12, where the subsequent new loading curve does not overlap completely with the unloading curve of the previous cycle. For example, the loading curve of cycle-1.0% is above the unloading curve of cycle-0.75%, and this small difference indicates that a (recoverable) elastic strain component makes up part of the imposed strain of 0.75%.

Another important aspect of fiber relaxation is the extent of it. It

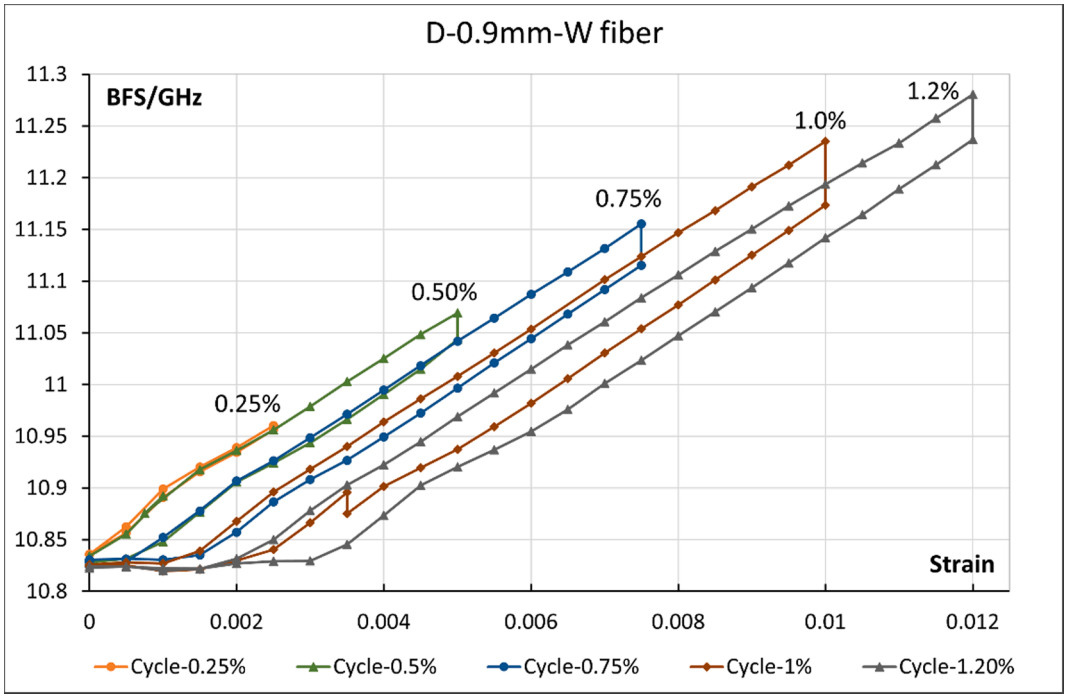

Fig. 12. Cyclic loading history of D-0.9 mm-W fiber.

should be noted that theoretically relaxation will never finish (as it is closely related to the theoretically never-ending creep behavior), but generally is proportional to log(t) and after a limited time period most of the relaxation has already occurred. Fig. 13 shows the measured BFS decrease (due to relaxation) as a function of ln(t) at an imposed strain of 1.0%. This BFS change is highly linear, and the predicted time-history curve of BFS decrease within a one-year period is shown in Fig. 14. It can be seen that within that period, for the D-2 mm-W fiber 50.5% of the total relaxation occurs on the first day, while 59.7% occurs within the first 3 days; and for the D-2 mm-Y fiber the corresponding percentages are 44.3% and 54.6%, respectively. Besides, the measurement results also show that for an imposed strain below 1.0% the magnitude of observed relaxation is smaller. For example, the BFS decrease of the D-0.9 mm-W fiber at 0.25% strain is about 6.5 MHz after 12 h and tends to be stable afterwards. Therefore, the results in this study show that in order to experimentally establish relaxation of at least 50% of the total that would occur over a year long period at high strain levels of 1.0%, a sustained tension test of about 2 days is needed.

4.3. A relaxation model for sensing fiber

Generally, the plastic strain of optical fibers comes from: (1) the inter-layer slippage due to interface debonding within the fiber cross-section, and (2) plastic deformation of the material itself (mainly the external jacket). According to the tension test results, it is reasonable to assume the plastic component corresponding to a certain imposed strain can be fully triggered and becomes a permanent residual strain when the fiber is fully unloaded to zero strain. Therefore, a fiber pre-tensioning to the anticipated maximum strain before fiber sensor installation will help to remove the error due to residual plastic strain in subsequent measurements. However, as elastic strain is dependent on the imposed fiber strain and elapsed time, it is important to properly model the elastic component and estimate the potential measurement error this may introduce.

Here a simplified model is proposed based on the tension test results in this study. Fig. 15 shows a typical hysteresis loop of a BFS-strain ($f-\varepsilon$) curve during a loading–unloading cycle. The fiber is first loaded (from zero strain) to a designated strain ε_m (shown in the loading curve O-P), and relaxation occurs over time, which results in a reduction of measured BFS, as shown by curve P-Q and Δf in Fig. 15. Finally, the measured BFS reaches a stable value (at point Q) which indicates the relaxation (corresponding to ε_m) process has finished. After that the fiber is unloaded to zero strain (see curve Q-R-O), and a residual strain is found which consist of a plastic ε_p and elastic component ε_e. If the fiber is loaded again from zero strain (from point O), the new loading will follow curve O-S-T, and it should be noted that new loading curve S-T is above the previous unloading curve Q-R, and the gap between them indicates the recoverable elastic component ε_e. According to the tension test results, it is reasonable to assume that afterwards the loading–unloading process (to a maximum strain of ε_m) will follow the narrow loop bounded by curve S-T-Q-R-S, and the geometry of this loop is determined by the fiber type (under the imposed strain ε_m). Therefore, this loop can be referred to as the "characteristic loop" of the optical fiber. It should be noted that after the loading–unloading cycle of ε_m, the strain sensing range of the fiber is reduced to $(\varepsilon_m - \varepsilon_p)$.

To better analyze the elastic strain behavior of optical fiber, the characteristic loop is moved to the origin (point S overlaps at point O), as shown in Fig. 16. For simplicity, the relation between elastic strain ε_e and the corresponding imposed strain ε is assumed to be linear, and hence the dotted line O-Q defines the ultimate BFS-strain curve when relaxation has finished, and this ultimate BFS-strain curve is used for strain interpretation of the fiber sensor. Accordingly, after rapid loading to point M (ε_1, f_1) with an imposed strain ε_1, the relaxation will finally result in a BFS decrease from f_1 to f_2 where a stable value is reached, see M−N in Fig. 16. In order to estimate the error, consider a rapidly imposed loading and unloading step at N (ε_1, f_2).

For this loading scenario, the maximum error occurs right after the loading stage when relaxation has not started to manifest yet, see Fig. 16. The maximum relative error is calculated below from the actual imposed strain $\Delta\varepsilon_1$ shown in Eq. (2),

$$\Delta\varepsilon_1 = \frac{\Delta f}{k_1} \tag{2}$$

The measured strain $\Delta\varepsilon_2$ as observed by the fiber sensor is expressed in Eq. (3),

$$\Delta\varepsilon_2 = \frac{\Delta f}{k_3} \tag{3}$$

where k_1 and k_3 are the gradient of rapid loading curve O-T (the upper boundary curve of the characteristic loop) and ultimate BFS-ε curve O-Q, respectively, see Fig. 16.

The maximum relative error (MRE) of measurement under loading conditions is deduced as Eq. (4):

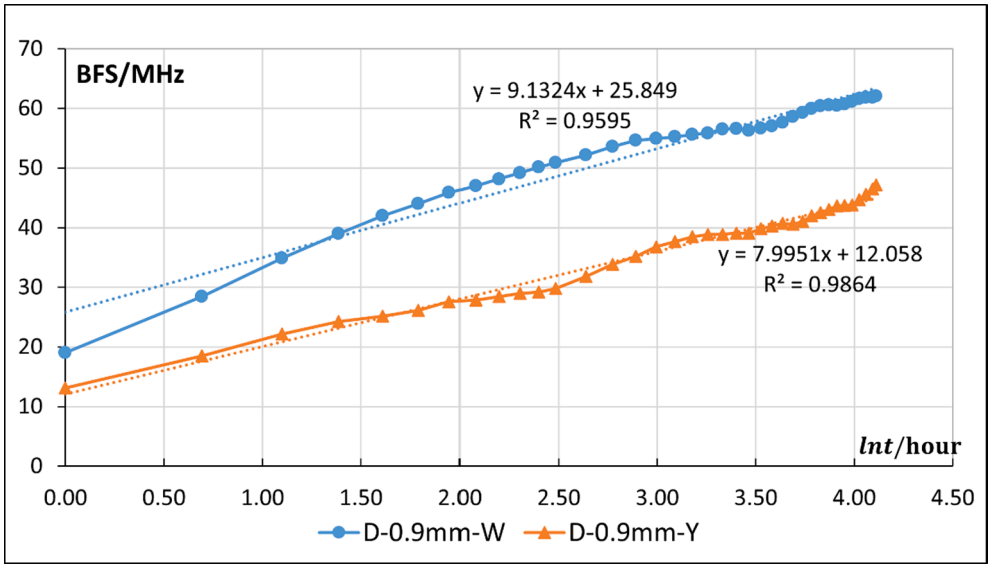

Fig. 13. BFS decrease due to relaxation (strain of 1.0%).

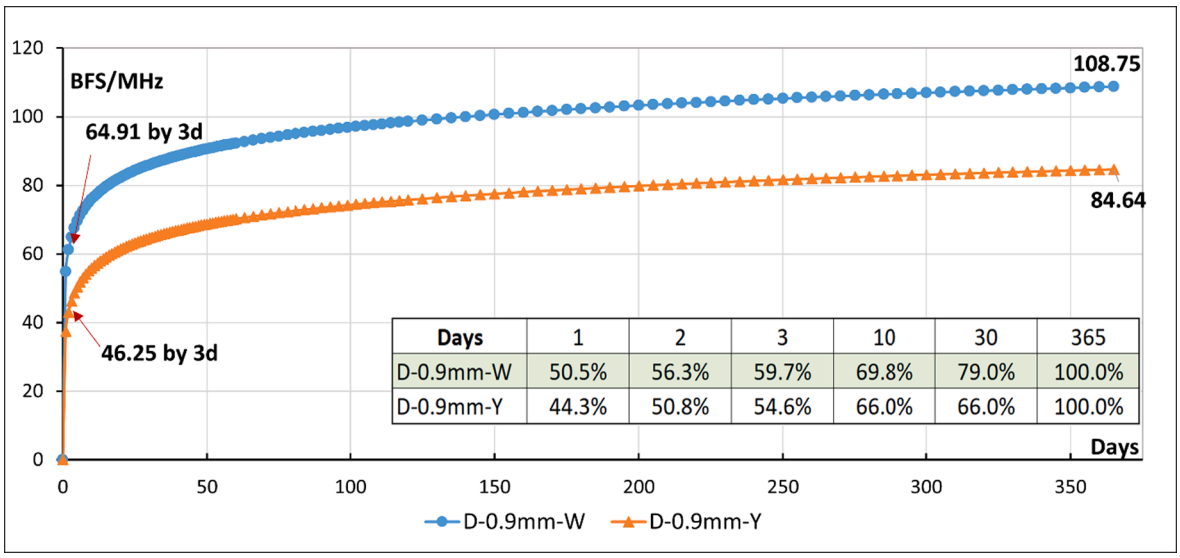

Days	1	2	3	10	30	365
D-0.9mm-W	50.5%	56.3%	59.7%	69.8%	79.0%	100.0%
D-0.9mm-Y	44.3%	50.8%	54.6%	66.0%	66.0%	100.0%

Fig. 14. Time-history of BFS decrease due to relaxation (strain of 1.0%).

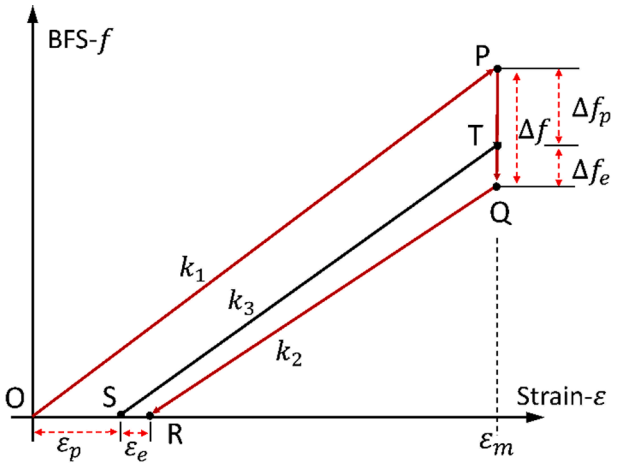

Fig. 15. Loop $f-\varepsilon$ curve of optical fiber under cyclic loading.

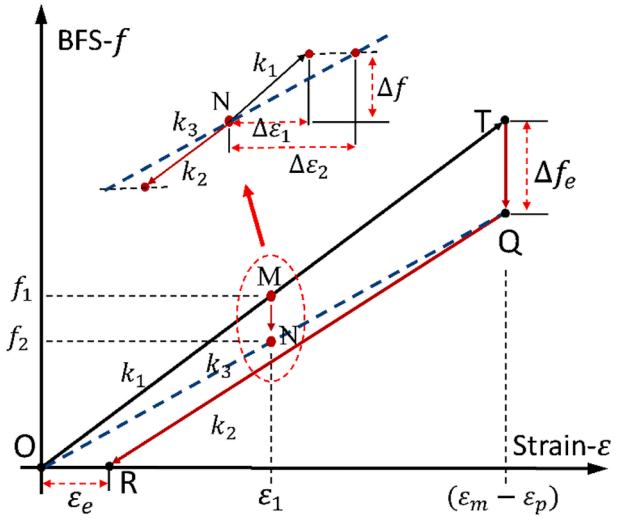

Fig. 16. Measurement error analysis based on characteristic loop.

$$MRE(load) = \frac{\Delta\varepsilon_2 - \Delta\varepsilon_1}{\Delta\varepsilon_1} = \frac{k_1 - k_3}{k_3} \tag{4}$$

From the above equation, the maximum relative error (MRE) of the optical fiber is decided by the gradients k_1 and k_3, which are related to the chacteristic loop, and hence determined by the fiber properties. Note that the measued Δf decreases with time due to relaxation, and the measured $\Delta\varepsilon_2$ will reduce gradually until to $\Delta\varepsilon_1$, which means over time the measurement error will decrease.

For the unloading scenario, the maximum error occurs right after the unloading when elastic bounce-back has not started yet. The maximum relative error in unloading MRE (unload) of measurement can be similarly deduced as in Eq. (5):

$$MRE(unload) = \frac{k_2 - k_3}{k_3} \tag{5}$$

where k_2 is the gradient of unloading curve R-Q (the lower boundary curve of the characteristic loop), see Fig. 16. It should be noted that for a fiber which exhibits relaxation, according to the fiber tension test in this study, there is a difference between k_1 and k_2 because the elastic component tends to bounce back slowly with reduced strain in the unloading process, and therefore k_1 is somewhat larger than k_2, while the difference is determined by the fiber type.

According to the proposed relaxation model and the characteristic loop, the maximum relative error (due to relaxation or creep) of the D-0.9 mm-W fiber and D-0.9 mm-Y fiber are calculated. The fiber is assumed to be first tensioned to 1% and hence plastic strain is triggered. After that the fiber is unloaded to zero strain, and reloaded to 1% again. By this pre-tensioning cycle the characteristic loop is obtained, but it should be noted that the maximum sensing strain of the fiber is reduced by removing the plastic strain. The results are shown in Table 2.

For the two D-0.9 mm fiber types, the MRE(load) of D-0.9 mm-W and D-0.9 mm-Y are 7.37% and −4.72%, respectively, while the MRE(unload) are much smaller at 3.0% and −1.93%, respectively. It can be

Table2
Maximum relative error of D-0.9 mm fiber.

Fiber Type	D-0.9 mm-W	D-0.9 mm-Y
k_1 (MHz/0.1%)	45.87	46.68
k_2 (MHz/0.1%)	44.00	48.04
k_3 (MHz/0.1%)	42.72	48.98
MRE (load)	7.37%	−4.72%
MRE (unload)	3.0%	−1.93%

concluded that after pre-tensioning, the error due to relaxation is limited for both fiber types. Besides, the positive MRE(load) and MRE(unload) for D-0.9 mm-W means most probably that the measured strain by DOFS is larger than the actual strain, while for D-0.9 mm-Y the negative values indicate the opposite. The results also show that the elastic strain component of D-0.9 mm-Y is very small as to be negligible, as for each loading cycle the accumulated strain is mostly the plastic component. As stated above, the proposed relaxation model predicts that the measurement error due to relaxation decreases over time, and the error values indicated here are therefore considered an upper bound estimate of the measurement error. Finally, it is highly suggested that pre-tensioning can effectively reduce the error due to relaxation (and creep) and therefore is a good way to process the sensing fiber before field installation.

5. Conclusion

A proper fiber selection for using distributed optical fiber sensor (DOFS) as a means to obtain point displacement measurements depends on understanding the general physical behavior of the optical fiber and selecting a fiber type with proper metrics for optimal sensing. Two fiber calibration tests, a combined tension test and a manual tension test, are proposed here to obtain the fiber properties. Based on the manual tension test results in this study, the influence of fiber relaxation is investigated, and a quantitative model is proposed that describes relaxation behavior and can be used to assess measurement errors. The main conclusions are summarized as follows:

(1) For the selection of sensing fibers in DOFS point-displacement measurements, the important metrics are: the physical structure of optical fiber, the maximum working strain (MWS), the limit strain, the relaxation behavior, the strain coefficient and the temperature coefficient. In addition, the axial stiffness is also an important metric when manual pre-tensioning is needed during sensor installation. An axial stiffness of no more than 3kN is suggested for manual pre-tensioning above 0.5% strain when used for point-displacement measurements.
(2) The mechanical properties of the optical fiber can be verified by a combined calibration test, preferably on a tension machine. The BFS-strain curve and axial stiffness can be obtained simultaneously in that way. In addition, a manual tension test also works for determining the properties of optical fibers with low axial stiffness, as shown in this study.
(3) The relaxation of optical fibers causes measurement errors and shall be checked prior to field installation. According to the experimental test results, relaxation of typical tight-buffered optical fibers (at a given primary imposed strain) generally consists of an (unrecoverable) plastic component and (recoverable) elastic component. The plastic component can be fully triggered and removed by beforehand pre-tensioning, and hence a pre-tensioning of the sensing fiber before installation can help reduce measurement errors caused by relaxation.
(4) The relaxation behavior can be described by the characteristic loop of the sensing fiber, and the maximum relative error of the measurement can be assessed accordingly. The proposed relaxation model can describe an upper bound estimate of measurement error quantitatively. The maximum (absolute) measurement errors of the D-0.9 mm-W and D-0.9 mm-Y fiber are 7.37% and 4.72% respectively.

DOFS is expected to gain increasing attention in field monitoring and will be more widely used in the future, but a proper fiber selection is key to successful and reliable measurements. This study provides insight into parameter verification of optical fibers.

CRediT authorship contribution statement

Xuehui Zhang: Conceptualization, Methodology, Investigation, Writing – original draft. **Wout Broere:** Supervision, Funding acquisition, Conceptualization, Writing – review & editing.

Declaration of Competing Interest

The authors declare that they have no known competing financial interests or personal relationships that could have appeared to influence the work reported in this paper.

Acknowledgements

This research has been financially supported by China Scholarship Council (China), Rijkswaterstaat, the Netherlands, and European Union's Horizon 2020 Research and Innovation Programme (Grant Number 723254).

References

[1] J.M. López-Higuera, L.R. Cobo, A.Q. Incera, A. Cobo, Fiber optic sensors in structural health monitoring, J. Lightwave Technol. 29 (4) (2011) 587–608, https://doi.org/10.1109/JLT.2011.2106479.
[2] E. Udd, W. Spillman, Fiber Optic Sensors: An Introduction for Engineers and Scientists, second ed., John Wiley & Sons Inc, New Jersey, 2011.
[3] A. Motil, A. Bergman, M. Tur, State of the art of Brillouin fiber-optic distributed sensing, Opt. Laser Technol. 78 (2016) 81–103, https://doi.org/10.1016/j.optlastec.2015.09.013.
[4] T. Horiguchi, K. Shimizu, T. Kurashima, M. Tateda, Y. Koyamada, Development of a distributed sensing technique using Brillouin scattering, J. Lightwave Technol. 13 (1995) 1296, https://doi.org/10.1109/50.400684.
[5] H. Ohno, H. Naruse, M. Kihara, A. Shimada, Industrial applications of the BOTDR optical fiber strain sensor, Opt. Fiber Technol. 7 (1) (2001) 45–64, https://doi.org/10.1006/ofte.2000.0344.
[6] C.K. Leung, K.T. Wan, D. Inaudi, X. Bao, W. Habel, Z. Zhou, M. Imai, Optical fiber sensors for civil engineering applications, Mater. Struct. 48 (4) (2015) 871–906, https://doi.org/10.1617/s11527-013-0201-7.
[7] T. Schwamb, K. Soga, R.J. Mair, M.Z.E.B. Elshafie, R. Sutherden, C. Boquet, J. Greenwood, Fibre optic monitoring of a deep circular excavation, Proc. Inst. Civil Eng. – Geotech. Eng. 167 (2) (2014) 144–154.
[8] M. Iten, A. Schmid, D. Hauswirth, A.M. Puzrin, Defining and monitoring of landslide boundaries using fiber optic systems, in: Int. Symp. on Prediction and Simulation Methods for Geohazard Mitigation, 2009, pp. 451–456.
[9] K. Soga, Understanding the real performance of geotechnical structures using an innovative fibre optic distributed strain measurement technology, Riv. Ital. Geotech. 4 (2014) 7–48. <https://associazionegeotecnica.it/wp-content/uploads/2017/05/rig_4_2014_soga-.pdf>.
[10] X. Wang, B. Shi, G. Wei, S.E. Chen, H. Zhu, T. Wang, Monitoring the behavior of segment joints in a shield tunnel using distributed fiber optic sensors, Struct. Control Health Monitor. 25 (1) (2018) e2056, https://doi.org/10.1002/stc.2056.
[11] H.F. Pei, J. Teng, J.H. Yin, R. Chen, A review of previous studies on the applications of optical fiber sensors in geotechnical health monitoring, Measurement 58 (2014) 207–214, https://doi.org/10.1016/j.measurement.2014.08.013.
[12] L. Pelecanos, K. Soga, M.Z. Elshafie, N. de Battista, C. Kechavarzi, C.Y. Gue, Y. Ouyang, H.J. Seo, Distributed fiber optic sensing of axially loaded bored piles, J. Geotech. Geoenviron. Eng. 144 (3) (2018) 04017122, https://doi.org/10.1061/(ASCE)GT.1943-5606.0001843.
[13] C.Y. Gue, M. Wilcock, M.M. Alhaddad, M.Z.E.B. Elshafie, K. Soga, R.J. Mair, The monitoring of an existing cast iron tunnel with distributed fibre optic sensing (DFOS), J. Civil Struct. Health Monit. 5 (2015) 573–586, https://doi.org/10.1007/s13349-015-0109-8.
[14] W. Liu, H. Zhou, B. Wang, Y. Zhao, Z. Leng, X. Chen, L. Li, S. Wang, Z. Chen, A subgrade cracking monitoring sensor based on optical fiber sensing technique, Struct. Control Health Monitor. 25 (9) (2018) e2213, https://doi.org/10.1002/stc.2213.
[15] G.S. Glaesemann, Optical fiber mechanical reliability, White Paper 8002 (2017) 1–62.
[16] P. Antunes, F. Domingues, M. Granada, P. André, Mechanical properties of optical fibers. INTECH Open Access Publisher, 2012. <https://pdfs.semanticscholar.org/e510/8ab03e34923f58d03585b316c870acce03f9.pdf>.
[17] Y. Ding, B. Shi, X. Bao, J. Gao, A study on the jacket effect of fiber optic sensors, in: Proc. SPIE 5579. Photonics North 2004: Photonic Applications in Telecommunications, Sensors, Software, and Lasers, Ottawa, Canada, 2004, pp. 43–45. <https://doi.org/10.1117/12.566581>.
[18] Z. Xu, F. Ansari, Measurement of creep of optical fiber by a low coherent white light double interferometer system, Sci. China Ser. E: Technol. Sci. 52 (3) (2009) 647–650, https://doi.org/10.1007/s11431-009-0066-8.

[19] S. Song, C. Yang, Z. Wu, Y. Zhang, S. Shen, Study on the creep properties of distributed optical fiber sensors, SPIE Smart Structures and Materials + Nondestructive Evaluation and Health Monitoring, SPIE, San Diego, California, United States, 2010, p. 76472M.
[20] W.N. Findley, F.A. Davis, Creep and relaxation of nonlinear viscoelastic materials, Courier corporation, 2013.
[21] M. Iten, D. Hauswirth, A.M. Puzrin, Distributed fiber optic sensor development, testing, and evaluation for geotechnical monitoring applications, Proc. SPIE 798207–7982015 (2011), https://doi.org/10.1117/12.881228.
[22] W. Lienhart, F. Moser, H. Schuller, T. Schachinger, Reinforced earth structures at Semmering base tunnel—construction and monitoring using fiber optic strain measurements. 10th International Conference on Geosynthetics (10ICG), 2014.
[23] Fibristerre, Information of BOFDA interrogator see, 2021. <https://www.fibristerre.de/files/BOFDA_distributed_fiber-optic_sensing.pdf> (latest accessed in September 2021).
[24] Corning optic fiber product information, 2021. <https://www.corning.com/media/worldwide/coc/documents/Fiber/PI-1463-AEN.pdf> (latest accessed in December 2021).